

## Expansion deformation and permeability characteristics of bituminous coal with different moisture content after CO<sub>2</sub> adsorption

Zhaolong Ge<sup>a,b,\*</sup>, Chengtian Li<sup>a,b</sup>, Zhe Zhou<sup>a,b</sup>, Xiangyu Zhang<sup>a,b</sup>, Yarui Guan<sup>a,b</sup>, Meiyu Sheng<sup>a,b</sup>

<sup>a</sup> State Key Laboratory of Coal Mine Disaster Dynamics and Control, Chongqing University, Chongqing, 400044, China

<sup>b</sup> School of Resources and Safety Engineering, Chongqing University, Chongqing, 400044, China



### ARTICLE INFO

**Keywords:**

Moisture content  
CO<sub>2</sub>  
Adsorption expansion  
Permeability change  
Porosity and minerals

### ABSTRACT

Injecting CO<sub>2</sub> into deep unexploitable coal seams is a means with dual benefits of enhanced coalbed methane exploitation (CO<sub>2</sub>-ECBM) and CO<sub>2</sub> geological storage (CGS). The permeability change of the coal seam after CO<sub>2</sub> injection is an important factor for the CO<sub>2</sub>-ECBM and CGS. However, the impact of the interaction of CO<sub>2</sub>-H<sub>2</sub>O-coal in the coal seam on the adsorption swelling and permeability characteristics is poorly understood. In this study, we quantitatively analyzed the adsorption characteristics, permeability characteristics, and microstructure changes of coal samples under CO<sub>2</sub>-H<sub>2</sub>O-coal interaction by Geotechnical Consulting & Testing Systems (GCTS), nuclear magnetic resonance (NMR), and X-ray diffraction (XRD). The results show that the increase of moisture content inhibits the adsorption of CO<sub>2</sub> due to the clusters formed by water molecules occupy the position of adsorption pores, reducing the expansion rate of coal samples. The reaction rate content of carbonate minerals in coal samples increases with the increase of moisture content after subcritical CO<sub>2</sub> treatment, leading to an increase in the relative content of clay minerals, which can enlarge the pore volume. However, the subcritical CO<sub>2</sub> treatment cannot completely eliminate the negative impact of loading and unloading processes on the mesopore and macropore, and therefore show a decrease of the pore volume and permeability. The dissolution of carbonate mineral in coal samples is more severe after supercritical CO<sub>2</sub> (ScCO<sub>2</sub>), which can effectively enlarge seepage pores and thus improves the permeability. The clay mineral content increases slightly at 5.6% moisture content, indicating that it also reacts significantly after ScCO<sub>2</sub> treatment. For instance, the permeability growth rate of 2.8% moisture content coal sample reaches 421.74% at 8 MPa effective stress, which is the best moisture content for permeability enhancement. In addition, the coal samples with 5.6% moisture content show the transformation from mesopores and macropores to micropores and small pores after subcritical CO<sub>2</sub> and ScCO<sub>2</sub> treatment, which provides more adsorption sites for CGS.

### 1. Introduction

Emission of greenhouse gases (GHGs), especially CO<sub>2</sub>, is considered as the main cause of global warming and climate change (Bachu, 2008). Carbon capture, utilization and storage (CCUS) is considered to be the most effective and feasible method to reduce carbon emissions and reduce the greenhouse effect (Zhang and Huisingsh, 2017). Compared with the complex and insecure deep-sea storage, geological storage is more promising and feasible. Salt-bearing layers, depleted oil reservoirs, unexploitable coal seams, basalt formations, and CO<sub>2</sub> hydrate are effective selections of underground CO<sub>2</sub> storage (Aminu et al., 2017). In particular, CO<sub>2</sub> injection into deep unexploitable coal seams has

improved the CGS and enhanced the coalbed methane recovery (CO<sub>2</sub>-ECBM), thus compensating the sequestration costs. It is considered as a geological reservoir with profitable application prospects (Leung et al., 2014; Mazzotti et al., 2009). At present, the technology has been successfully tested in several countries, including the USA, Canada, China, and Japan (Fujioka et al., 2010; Gunter et al., 1997; Pashin et al., 2015; Wong et al., 2007).

Coal seam permeability is one of the most important factors that affect ECBM and CGS. The permeability is controlled by several factors, including temperature, stress, moisture, and coal type (Cui et al., 2021; Wang et al., 2017; Zhu et al., 2020). The CO<sub>2</sub> injection into coal seam will cause the expansion and deformation of the coal seam, and will thus

\* Corresponding author. State Key Laboratory of Coal Mine Disaster Dynamics and Control, Chongqing University, Chongqing, 400044, China.

E-mail address: [gezhaolong@cqu.edu.cn](mailto:gezhaolong@cqu.edu.cn) (Z. Ge).

induce a change of the permeability. Therefore, it is necessary to study the processes that control the adsorption expansion and the permeability change of the coal seam that are caused by the CO<sub>2</sub>-H<sub>2</sub>O-coal interaction under CO<sub>2</sub> injection. These studies will constitute the basis for predicting the impact of CO<sub>2</sub> injection on the permeability characteristics of the coal seam and will provide reference data for ECBM and CGS. Jasinge et al. and Niu et al. (Jasinge et al., 2012; Niu et al., 2017) conducted permeability tests on raw coal and briquette coal prior and after CO<sub>2</sub> injection, respectively, and recognized that CO<sub>2</sub> adsorption expansion is unfavorable to permeability. Moreover, they detected a well-defined correlation between expansion and permeability. Perera et al. (2011) studied the effect of subcritical and ScCO<sub>2</sub> on coal swelling and permeability through CO<sub>2</sub> adsorption experiments at different pressures. They found that the swelling caused by ScCO<sub>2</sub> adsorption was about two times higher than that of subcritical CO<sub>2</sub>, and the permeability decreases with the increase of CO<sub>2</sub> injection pressure. Niu et al. (2018) studied the effect of CO<sub>2</sub> adsorption on coal anisotropy by comparing the changes of coal three-dimensional permeability before and after CO<sub>2</sub> adsorption. They concluded that the CO<sub>2</sub> adsorption, especially ScCO<sub>2</sub>, enhanced the permeability anisotropy of coal due to the high adsorption sensitivity of low permeable cleat and the low adsorption sensitivity of high permeable bedding. Based on the measured free swelling strain of rock samples, Shi et al. (2014) established a new expansion strain-permeability model to predict the permeability response of rock core to binary gas mixture. Li et al. (2019) investigated the response of coal permeability and pore distribution to ScCO<sub>2</sub> adsorption by means of permeability measurement and Mercury intrusion porosimetry (MIP). They confirmed that ScCO<sub>2</sub> adsorption is conducive to the formation and connection of mesopores and macropores in coal, which increases the permeability. These previous studies have documented the link between coal expansion and permeability after CO<sub>2</sub> adsorption. However, the moisture in the coal seam that will exert a major impact on the adsorption and permeability characteristics was not considered in the previous studies (Liu et al., 2022).

The former studies have documented that CO<sub>2</sub> adsorption not only caused expansion deformation, but also complex geophysical, mineralogical, and chemical reactions, including extraction and dissolution of minerals of the coals. These processes change the original mineral composition, pore distribution, and permeability of the coal (Gao et al., 2022; Song et al., 2020; Xu et al., 2017; Zhang et al., 2019). Cheng et al. (2021) treated coal samples with subcritical and ScCO<sub>2</sub>, respectively, and measured the mineral composition and pore structure by XRD and mercury intrusion porosimetry. They recognized that the proportions of kaolinite and quartz in the coal samples were significantly reduced after the treatment. They proposed that ScCO<sub>2</sub> changes the chemical structure of the coal surface, thus affecting the porosity and pore volume of the coal. H. Zhang et al. (2021) and Hu et al. (2021) conducted ScCO<sub>2</sub> exposure experiments on different coal ranks and detected changes of their pores. They found that the long-term ScCO<sub>2</sub>-H<sub>2</sub>O interaction causes the reduction of mesopores in coal samples, whereas the effect on micropores is minor. The authors proposed that this will further affect the adsorption capacity of coal samples. Wang et al. (X. Wang et al., 2021) studied the effects of acidic and alkaline solutions on the adsorption capacity of coal and found that the large amount of dissolution of minerals in acidic environments improves the adsorption capacity of coal. In addition, the impact of water on the minerals, pores, adsorption capacity, and permeability of coal were analyzed by establishing a fully coupled multi-physical model of coal deformation, gas flow, and water loss. Teng et al. (2017) recognized that moisture loss would increase the porosity and permeability of coal. Du et al. (2020) used mercury intrusion method to analyze the pores of coal samples prior to and after ScCO<sub>2</sub>-H<sub>2</sub>O treatment, and detected that the partial corrosion of calcite cracks caused a major increase of the macropore volume by 545% at 1000m depth and 1058% at 2000m depth. The data indicate that ScCO<sub>2</sub>-H<sub>2</sub>O treatment can expand pores and fractures and also increases the pore connectivity. Massarotto et al. (2010) analyzed the elemental

composition of coal samples treated with ScCO<sub>2</sub>-H<sub>2</sub>O and recognized that effect of ScCO<sub>2</sub>-H<sub>2</sub>O significantly decreases Ca content and achieves coal seam permeability enhancement. Li et al. (2022) studied the effect of moisture on the pore distribution and mineral composition after ScCO<sub>2</sub> injection into coal samples and founded that the mineral content decreased with the increase of water content, which was caused by the dissolution of clay minerals in acidic environments. In contrast, the volume of transition pore, mesopore, and macropore reached the maximum value when the moisture content was 3.82%, indicating differing effects of ScCO<sub>2</sub>-H<sub>2</sub>O for respective pore sizes. The previous studies mostly focused on the influence of moisture on the microstructure of coal samples, but the influence of the microstructure change on the permeability and adsorption characteristics of coal seams was not considered.

In this paper, we present the results of subcritical and ScCO<sub>2</sub> adsorption and seepage experiments that we have conducted on coal samples with different moisture contents. We used GCTS, NMR, and XRD to obtain the adsorption expansion principles and permeability characteristics of the coal samples under CO<sub>2</sub>-H<sub>2</sub>O-coal interaction. The pore structure and mineral composition prior to and after the experiment were analyzed to reveal the change principles of the pore structure and mineral composition. Subsequently, the interaction mechanism of CO<sub>2</sub>-H<sub>2</sub>O-coal and its influence on the expansion and seepage characteristics of coal seams are established, providing an important reference for ECBM and CGS.

## 2. Sample material and experimental background

### 2.1. Samples and sample preparation

The coal samples used in this study were collected from Shenshu coal mine, Yulin City, Shaanxi Province, China (Fig. 1). In order to reduce the influence of the differences of coal samples on the experimental results, all coal samples were taken from the same coal block along the same horizontal bedding direction (Wang et al., 2022), and processed into standard cylindrical coal samples of 50mm × 100 mm according to the standards of the International Association of Rock Mechanics. In order to ensure the accuracy and validity of the experimental data, each sequence of the experiments was repeated three times, and the average value was regarded as the final result.

The coal sample was dried at 110 °C for 24 h before the experiments, and the dry weight was measured to determine the saturated moisture content. The average saturated moisture content of the coal samples is 11.20%. In order to study the effect of CO<sub>2</sub> adsorption on permeability of coal with different moisture contents, five different moisture contents were used in this study according to the average saturated moisture content. Since the pore structure of coal samples may be damaged during the loading and unloading process, group M were set up for comparison in this study. Except for no CO<sub>2</sub> adsorption, the remaining operations are exactly the same to study the damage of the pores and fissures of the coal samples during the test. The sample numbers are shown in Table 1. The moisture content in Table 1 is calculated by the formula:

$$\omega = \frac{G_w}{G_s} \times 100\% \quad (1)$$

where  $\omega$  is the moisture content (in %), G<sub>w</sub> is the weight of moisture in the pores of the coal sample (in g), and G<sub>s</sub> is the weight of the dried coal sample (in g).

### 2.2. Experimental principle

Our experiment adopts the steady state test method. For compressible gases, fluid expansion can affect the permeability measurements. Assuming that the permeation of gas through the sample is an isothermal

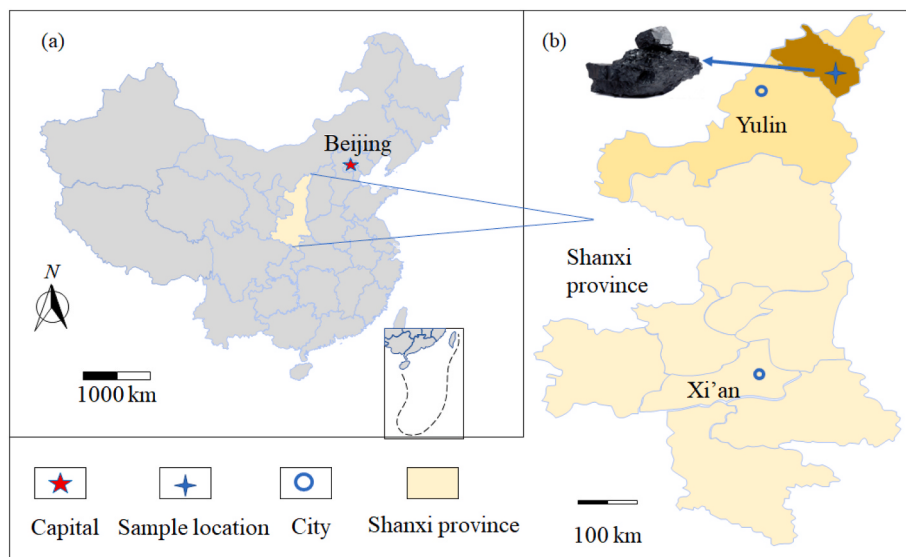


**Fig. 1.** Location of the studied samples.

**Table 1**  
Samples and experimental conditions.

Sample number	Moisture content (%)	CO <sub>2</sub> adsorption pressure (MPa)	Temperature (°C)
A1	0.00	4	35
B1	0.00	8	35
A2	2.80	4	35
B2	2.80	8	35
A3	5.60	4	35
B3	5.60	8	35
A4	8.40	4	35
B4	8.40	8	35
A5	11.20	4	35
B5	11.20	8	35
M	0.00	–	35

process and follows the ideal gas principles, the gas permeability can be calculated according to Darcy's law:

$$K = \frac{2\mu P_a LQ}{A(P_1^2 - P_2^2)} \quad (2)$$

where  $k$  is the permeability (in mD),  $Q$  is gas flow rate (in cm<sup>3</sup>/s),  $P_a$  is the atmospheric pressure (0.1 MPa),  $A$  is the cross-sectional area of the sample (in cm<sup>2</sup>),  $L$  is the sample length (in m),  $P_1$  is the inlet pressure (in MPa),  $P_2$  is the outlet gas pressure (in MPa), and  $\mu$  is the gas viscosity (in MPa·s).

In order to study the permeability changes of different deep coal seams after CO<sub>2</sub> injection, the seepage tests at the effective stress of 3–8 MPa were carried out in this paper. And the seepage experiments were conducted under different stress conditions of axial pressure of 2.8 MPa–7.8 MPa and confining pressure of 5.5 MPa–10.5 MPa. The pressure of injected He gas was kept at 3.1 MPa to study the permeability change under different effective stress. According to the Terzaghi effective stress formula, the effective stress acting on the coal sample can be expressed as:

$$\sigma_e = \frac{1}{3}(\sigma_a + 2\sigma_c) - \frac{1}{2}(P_1 + P_2) \quad (3)$$

where  $\sigma_e$  is the mean effective stress (in MPa),  $\sigma_a$  is the axial stress (in MPa),  $\sigma_c$  is the effective radial stress (in MPa),  $P_1$  is the inlet pressure (in MPa),  $P_2$  is the outlet pressure (in MPa).

### 2.3. Analytical procedure

Three permeability measurements were conducted before and after CO<sub>2</sub> adsorption and desorption by using He as the seepage gas. The changes of the permeability before and after CO<sub>2</sub> adsorption were compared to study the effect of swelling deformation on the permeability of the coal samples. The change of permeability after CO<sub>2</sub> desorption was analyzed to investigate the impact of CO<sub>2</sub>–H<sub>2</sub>O–coal interaction on the permeability of the coal samples. In addition, NMR tests were conducted before CO<sub>2</sub> adsorption and after CO<sub>2</sub> desorption to study the modification of the coal pore structure by CO<sub>2</sub>–H<sub>2</sub>O–coal during CO<sub>2</sub> adsorption. The analytical procedure is summarized in Fig. 2.

We measured the permeability of coal samples before and after CO<sub>2</sub> adsorption and CO<sub>2</sub> desorption with the triaxial test system for dynamic and static rocks at high temperature and pressure, made by Geotechnical Consulting & Testing Systems (GCTS) of the State Key Laboratory of Coal Mine Disaster Dynamics and Control at Chongqing University. The device with a maximum axial pressure of 3000 KN, a confining pressure of 210 MPa, and a maximum temperature of 200 °C, composed of gas supply system, a geological environment simulation system, and a data acquisition system. The equipment can automatically warm up and maintains a constant temperature during the test. The two-way deformation during the CO<sub>2</sub> adsorption process is measured by axial and circumferential extensometers with a deformation measurement range of ±6 mm. The data acquisition system records stress, temperature, micro-strain in real time and processes the experimental results. A vacuum pump was used to discharge the residual gas. A schematic diagram of the specific test device is shown in Fig. 3.

A layer of 704 silicone rubber was applied on the side of the coal sample to ensure the accuracy of the permeability analyses. Air leak tests were conducted according to the Chinese Energy Industry Standard NB/T 47013.8–2012 to ensure that all tests are performed under non-leakage conditions. The impact of the moisture content and gas adsorption on the permeability was studied in the experiments. During the gas adsorption process, the temperature was controlled at 35 °C, the axial stress was 10 MPa, and the radial stress was 10 MPa, simulating the natural conditions at a depth of 1000 m (Du et al., 2020). The studies previous show that the maximum expansion of coals caused by CO<sub>2</sub> adsorption occurs within 3–4 h after adsorption, and the reaction rate decrease with time. Therefore, 6 h CO<sub>2</sub> adsorption is conducted in this paper which is sufficient to explore the influence of CO<sub>2</sub>–H<sub>2</sub>O–coal reaction (Perera et al., 2011). The pressures of CO<sub>2</sub> injection are 4 MPa and

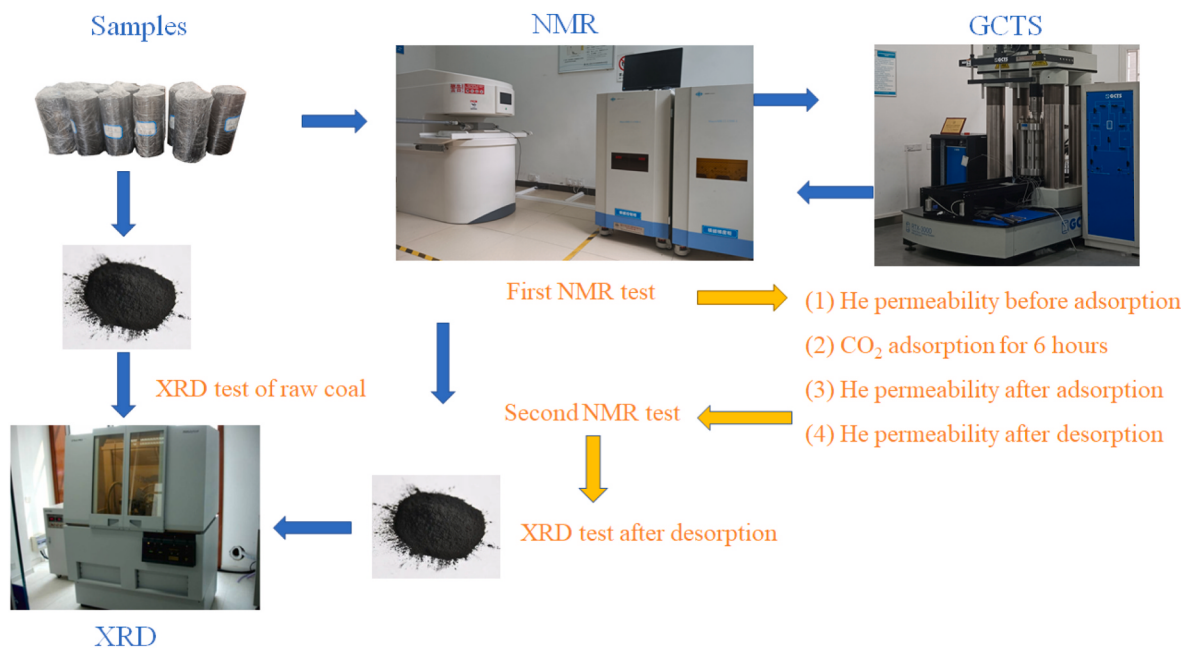


**Fig. 2.** Outline of the analytical procedure.

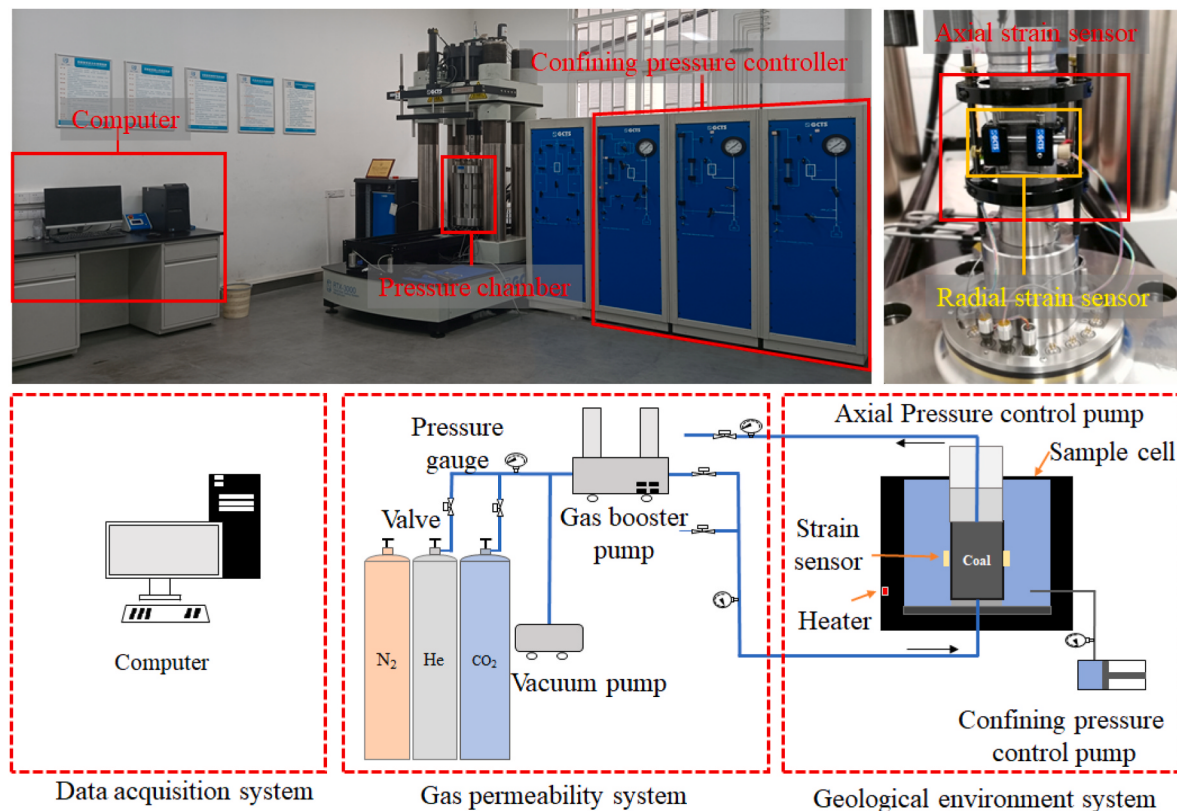


**Fig. 3.** Scheme of the adsorption and seepage device.

8 MPa, representing the adsorption of subcritical and ScCO<sub>2</sub>, respectively. The specific procedures are as follows: (1) Loading of the coal sample into the chamber and installation of the auxiliary devices, (2) Keeping the temperature constant and injecting He to measure the permeability under different effective stress before CO<sub>2</sub> adsorption, (3) Keeping the stress and the temperature at constant 10 MPa and 35 °C, respectively, and injecting CO<sub>2</sub> for saturated adsorption for 6 h after

vacuuming, (4) Injecting He again to measure the permeability under different effective stress after CO<sub>2</sub> saturated adsorption, (5) Removing the coal sample and repeating (1) and (2) to measure the permeability after complete desorption for 72 h.

### 3. Results

#### 3.1. Adsorption-swelling characteristics of coal sample

The swelling strain at different adsorption pressures is shown in Fig. 4 which indicates that the axial strain, radial strain, and volume strain of the coal samples decrease continuously with the increase of moisture content. After subcritical  $\text{CO}_2$  adsorption, the volume strain rate of the coal sample decreased from 2.28% of dry coal to 0.22% of water-saturated coal, documenting the decrease with the increase of the moisture content. Similarly, the volume strain decreased from 3.01% for dry coal to 0.44% for water-saturated coal samples after  $\text{ScCO}_2$  adsorption. The results show that the moisture content of the coal sample is negatively correlated with its swelling strain at a constant adsorption pressure, which is consistent with the previous data (Cai et al., 2013; Hao et al., 2018). In addition, Jin and Wang (Jin et al., 2017; X. Wang et al., 2021) point out that at low water content, water molecules adsorb in micropores and small pores, competing with  $\text{CO}_2$  adsorption. Huang et al. (2018) think that water molecules in coal preferentially adsorb on sulfur- and oxygen-containing groups at low moisture conditions, while migrate and accumulate in the middle of accessible pores at high moisture conditions, which occupies the spatial position of  $\text{CO}_2$  in the macropore and fractures, inhibiting the adsorption expansion of coal.

Fig. 4 illustrates that the volume strain of the coal samples decreased by 0.78%, 0.54%, 0.24%, and 0.50% with the increase of water content after subcritical  $\text{CO}_2$  saturated adsorption, respectively. The volume swelling of coal samples decreased by 0.97%, 0.79%, 0.25%, and 0.56% after  $\text{ScCO}_2$  saturated adsorption respectively. Both show a trend of first decreasing and then increasing. The reduction rate of the volume strain reached a minimum at the interval of the water content increasing from 5.6% to 8.4%.

#### 3.2. Seepage characteristics

##### 3.2.1. Permeability before $\text{CO}_2$ adsorption

The permeability of the coal samples prior to  $\text{CO}_2$  adsorption was analyzed and the results are illustrated in Fig. 5. As shown in Fig. 5, the permeability of coal samples before  $\text{CO}_2$  adsorption is controlled by the moisture content. The permeability decreases rapidly at first and then slowly as the increase of moisture content. The reasons of the permeability decrease are as followed: (1) Water rapidly fills into the inorganic pores of coal samples through capillary force, and adsorbs on the pore surface through intermolecular force, which cause clay minerals and

coal matrix expand and compresses the seepage channel. (2) water blocks the seepage channel such as pore throat, resulting in the reduction of permeability (Meng and Li, 2013). However, this effect is weakened with the continuous increase of water content, which causes the permeability decay rate of coal samples fast at first and then slow. The result is consistent with the study previous (Talapatra and Karim, 2020).

At the same time, the relationship between permeability and effective stress is shown in Fig. 6. The permeability of coal samples decreases continuously as the effective stress increases. This is caused by the narrow and even close of seepage channel of coal sample with the effective stress increases, which is consistent with the studies previous (Guo et al., 2014; Meng et al., 2015; Meng and Li, 2013).

##### 3.2.2. Permeability after adsorption

Seepage experiments after  $\text{CO}_2$  adsorption at different effective stress and with varying moisture content were conducted to study the effect of  $\text{CO}_2$  adsorption (group A for 4 MPa, group B for 8 MPa) on the permeability of the coal samples. The results are shown in Fig. 7. The diagrams indicate that the permeability of the coal samples with different moisture contents decreases to different degrees after  $\text{CO}_2$  saturation adsorption. According to the permeability before and after  $\text{CO}_2$  adsorption, we define the permeability adsorption loss rate ( $K_a$ ) as (Niu et al., 2019):

$$K_a = \frac{K_0 - K_1}{K_0} \times 100\% \quad (4)$$

Where  $K_a$  is the permeability before  $\text{CO}_2$  adsorption and  $K_1$  is the permeability after saturated adsorption of  $\text{CO}_2$ .

According to Fig. 8, the  $K_a$  values of the dry coal samples after subcritical  $\text{CO}_2$  treatment are 43.57%, 40.57%, 35.38%, 28.69%, and 20.39% with the effective stress increase, respectively (Fig. 8a) and the  $K_a$  values after  $\text{ScCO}_2$  treatment increase to 63.70%, 59.92%, 55.49%, 55.59%, 48.61%, and 41.18%, respectively (Fig. 8b). The coal samples with other moisture contents show a similar attenuation law. We propose that the permeability of the coal samples with different moisture contents is attenuated to different degrees after the adsorption saturation of subcritical and  $\text{ScCO}_2$ , and the degree of attenuation decreases continuously with the increase of the effective stress, i.e.,  $\text{CO}_2$  adsorption has a minor effect on the coal permeability attenuation under high stress conditions (deep geological conditions).

Moreover, Fig. 8a shows that the permeability of coal samples decreases to different extent with the change of moisture content after subcritical  $\text{CO}_2$  saturation adsorption. Taking the effective stress of 3

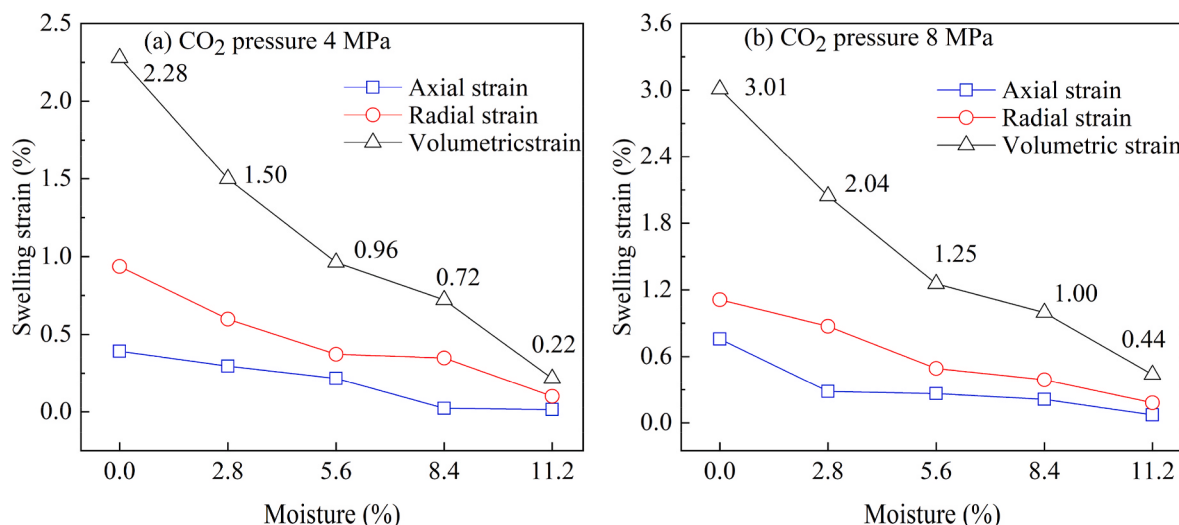
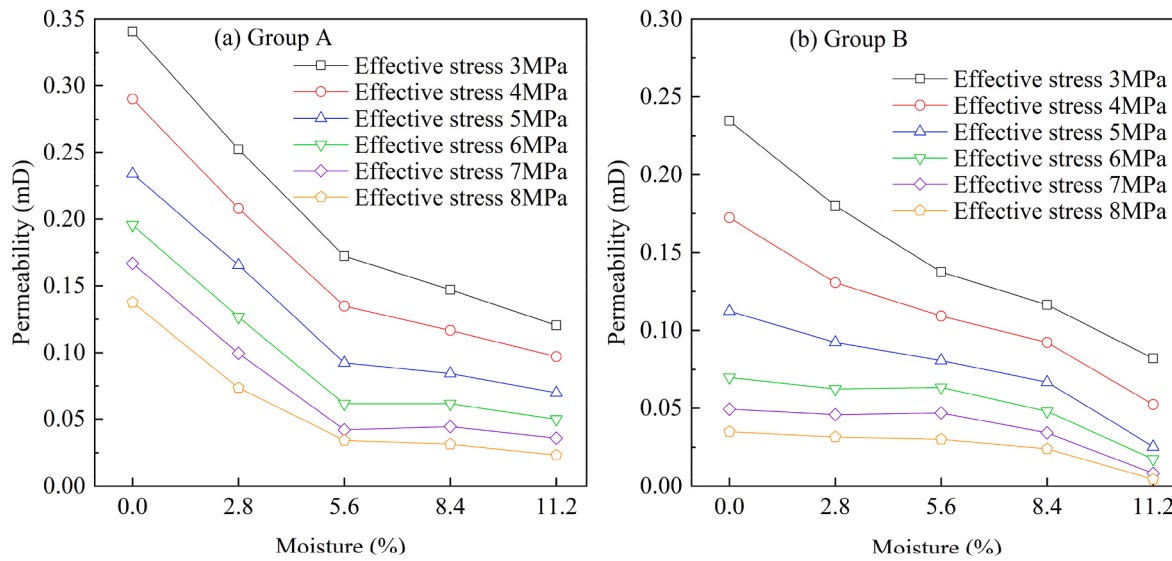
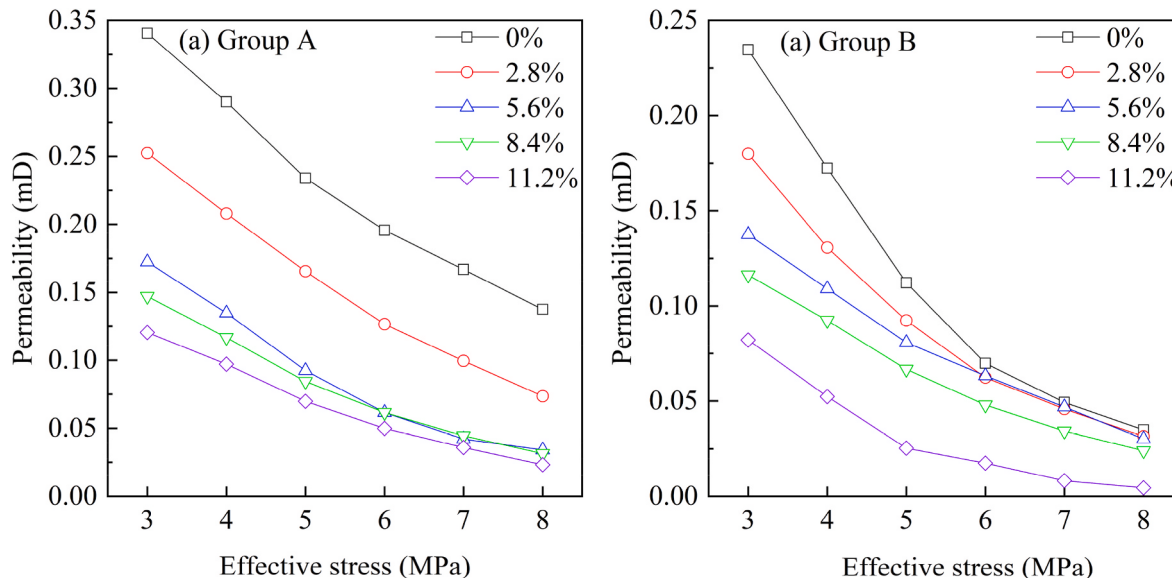


Fig. 4. The swelling strain with different moisture content after  $\text{CO}_2$  adsorption.



**Fig. 5.** Link between permeability of the coal samples and moisture content before adsorption at (a) group A and (b) group B.



**Fig. 6.** Link between permeability of the coal samples and effective stress before adsorption at (a) group A and (b) group B.

MPa as an example, the permeability of the coal samples with different moisture content attenuates by 43.57%, 61.79%, 69.44%, 60.30%, and 56.82%, respectively. The  $K_a$  values increase at low moisture contents but decrease at higher moisture content. The attenuation degree is the smallest for a moisture content of 0%. The permeability decay of coal samples shows a similar behavior under other effective stresses. Correspondingly, as shown in Fig. 8b, the permeability attenuation of coal samples with increasing moisture content reached 63.70%, 62.74%, 68.91%, 75.88%, and 72.09% (again for 3 MPa effective stress) after  $\text{ScCO}_2$  saturated adsorption, thus showing the same trend of decrease at first and subsequent increase. The lowest attenuation degree is obtained for a moisture content of 2.8%.

As shown in Fig. 8, comparing the permeability changes after subcritical and  $\text{ScCO}_2$  adsorption, it can be seen that the  $K_a$  after  $\text{ScCO}_2$  adsorption tends to be higher. Because the adsorption capacity is greater and the matrix expands more due to the higher pressure of supercritical  $\text{CO}_2$ , resulting in greater compression of the seepage channel.

### 3.2.3. Permeability after desorption

The interaction of the  $\text{CO}_2\text{-H}_2\text{O}$ -coal matrix induces complex geochemical modifications when  $\text{CO}_2$  is injected into the water-bearing coal seam, which, in turn, change the seepage characteristics of the coal seam (Du et al., 2018). The permeability of the coal samples after the  $\text{CO}_2$  desorption (group A for 4 MPa, group B for 8 MPa) is shown in Fig. 9. The diagrams show that the permeability of the coal sample cannot be completely recovered after subcritical  $\text{CO}_2$  desorption, as the permeability of the coal samples is mostly higher than the initial permeability (Fig. 9b), showing an immense difference.

According to the permeability changes before adsorption and after desorption, the permeability increase rate is defined as:

$$K_b = \frac{K'_1 - K_0}{K_0} \times 100\% \quad (5)$$

where  $K_b$  is the permeability before gas adsorption and  $K'_1$  the permeability after complete  $\text{CO}_2$  desorption.

Fig. 10 shows the permeability increase rate of coal samples after

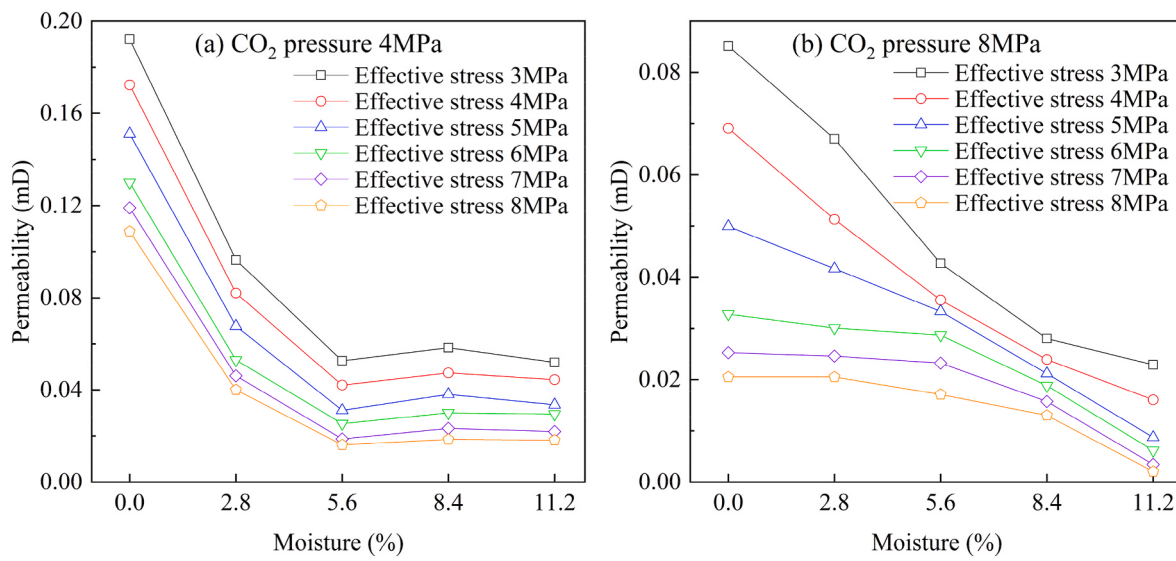


Fig. 7. The permeability of coal samples with different moisture content after adsorption at a  $\text{CO}_2$  pressure of (a) 4 MPa and (b) 8 MPa.

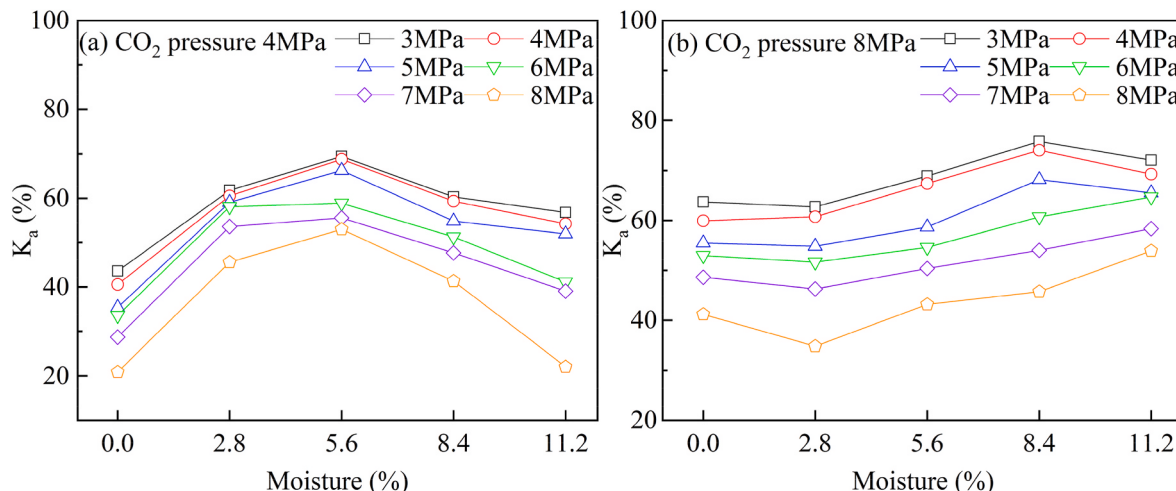


Fig. 8. The permeability adsorption loss rate ( $K_a$ ) of coal samples after adsorption at a  $\text{CO}_2$  pressure of (a) 4 MPa and (b) 8 MPa.

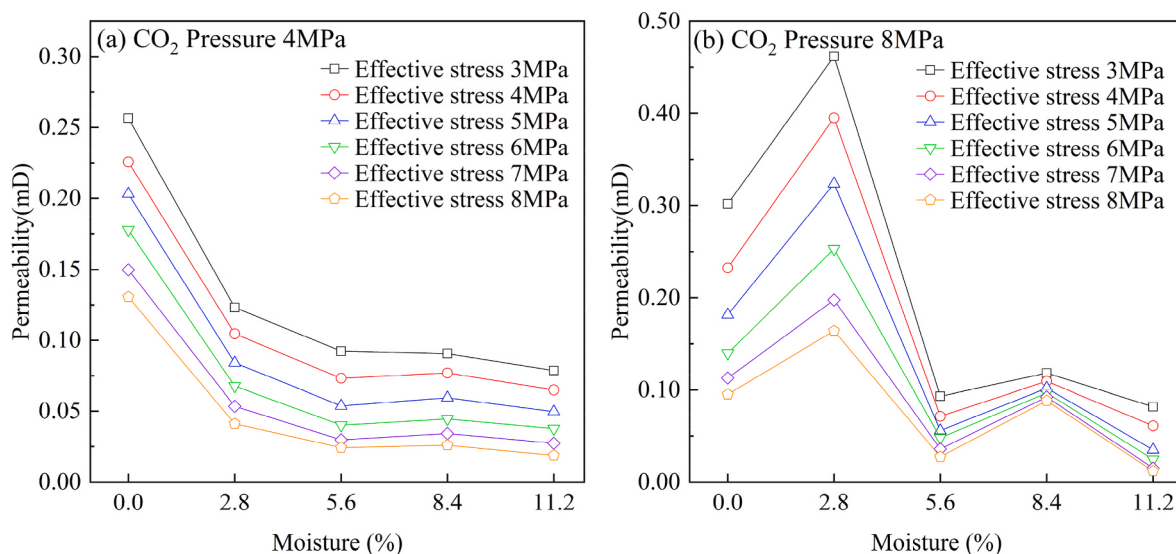
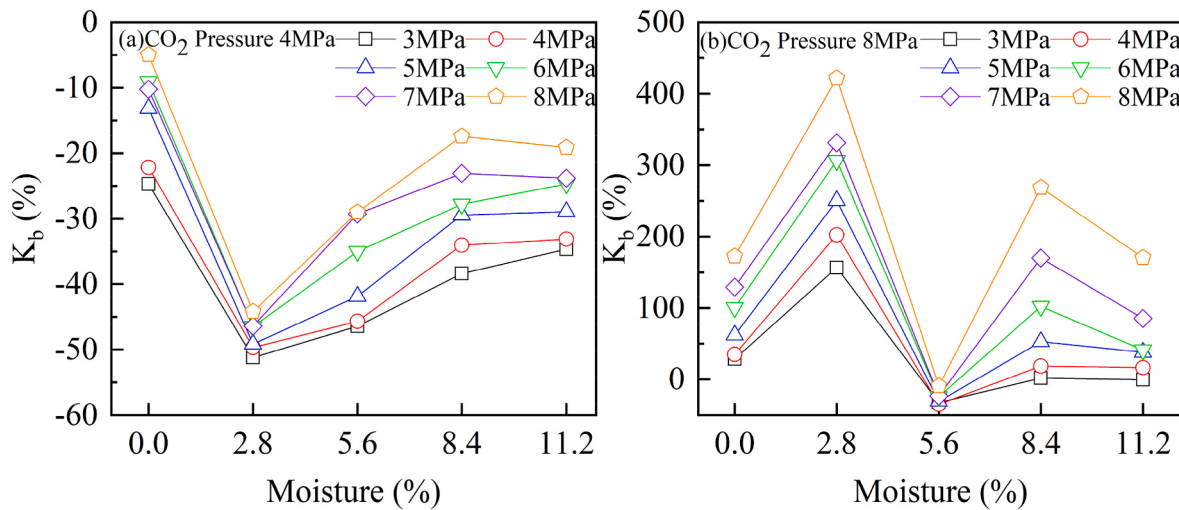


Fig. 9. The permeability of coal samples with different moisture content after desorption at a  $\text{CO}_2$  pressure of (a) 4 MPa and (b) 8 MPa.



**Fig. 10.** The permeability increase rate ( $K_b$ ) of coal samples with different moisture content after desorption at a  $\text{CO}_2$  pressure of (a) 4 MPa and (b) 8 MPa.

subcritical  $\text{CO}_2$  is fully desorbed. The diagrams indicate that the permeability of the coal sample appears to be attenuated after  $\text{CO}_2$  desorption, and the attenuation degree decreases with the increase of the effective stress. This is consistent with the permeability attenuation principles after adsorption proposed in previous text.

As shown in Fig. 10a,  $K_b$  reaches values of  $-24.70\%$ ,  $-51.22\%$ ,  $-46.43\%$ ,  $-38.37\%$ ,  $-34.66\%$  (for 3 MPa effective stress) with the increase of the coal sample moisture content after subcritical  $\text{CO}_2$  desorption, with showing a decrease at first that followed by an increase. For a moisture content of 2.8% the attenuation degree is the largest. Different from subcritical  $\text{CO}_2$  desorption, the permeability of coal samples is mostly higher than the initial permeability after  $\text{ScCO}_2$  desorption (Fig. 10b). The  $K_b$  of coal samples with different moisture contents are  $28.57\%$ ,  $156.65\%$ ,  $-32.34\%$ ,  $1.76\%$ , and  $-0.42\%$ , respectively (for 3 MPa effective stress). Except for the coal sample with a water content of 5.6%, the permeability of the coal samples increased. The permeability of the saturated coal sample with 5.6% a water content slightly decreased under the effective stress of 3 MPa. The  $K_b$  reaches a maximum of  $156.65\%$  for a moisture content of 2.8%. The  $K_b$  values of the coal sample with a moisture content of 2.8% are  $156.65\%$ ,  $202.36\%$ ,  $250.37\%$ ,  $306.59\%$ ,  $331.34\%$ , and  $421.74\%$ , respectively with increase of the effective stress. Similarly, the  $K_b$  of coal samples with moisture content of 0%, 8.4%, and 11.2% increased from  $28.57\%$ ,  $1.76\%$ , and  $-0.42\%$  of the 3 MPa effective stress to  $172.54\%$ ,  $268.57\%$ , and  $170.56\%$  of the 8 MPa effective stress, respectively. The results show that  $\text{ScCO}_2$  can effectively enhance the permeability of coal samples that is further improved by high stress conditions.

Unexpectedly, the  $K_b$  of the 5.6% moisture content coal sample under different effective stresses were  $-32.34\%$ ,  $-34.80\%$ ,  $-33.93\%$ ,  $-24.32\%$ ,  $-23.36\%$ , and  $-9.09\%$  after supercritical  $\text{CO}_2$  desorption. Thus, the permeability after desorption was lower than the initial permeability, which is consistent with the trend of coal samples treated with subcritical  $\text{CO}_2$ . This fact may be the result of the transformation and collapse of seepage pores during  $\text{CO}_2$  adsorption. Therefore, is necessary to specifically study the pores of coal samples before and after adsorption.

### 3.3. Pore distribution

Coal is a natural organic rock with a complex pore structure. The internal pores are the main sites for the adsorption and migration of  $\text{CO}_2$  and coalbed methane. Based on their size coal pores can be divided into micropores ( $<10$  nm), small pores ( $10\text{--}100$  nm), mesopores ( $100\text{--}1000$  nm), and macropores ( $>1000$  nm). Micropores and small pores are considered to be the main sites for adsorption, whereas

mesopores and macropores are classified as seepage pores (Li et al., 2022; Liu et al., 2020).

In this study, NMR tests were performed on coal samples before adsorption and after desorption, in order to explore the effect of  $\text{CO}_2$  injection on the pores of the coal samples. Since the pore distribution of coal samples may change during the loading and unloading process, the M group coal samples were additionally analyzed twice by NMR to eliminate their influence on pores (N. Danesh et al., 2017). As shown in Fig. 11, the experiments results indicate that the pores of the group M coal samples transformed from mesopores and macropores to micropores and small pores after the treatment. The volumes of micropores, small pores, mesopores, and macropores of the coal samples changed by 0.0508, 0.1147,  $-0.0715$ , and  $-0.1616$ , respectively.

The T2 distribution of coal samples with different moisture contents before and after subcritical  $\text{CO}_2$  adsorption is shown in Fig. 12. All kinds of pores are developed in coal samples, with micropores and small pores accounting for more than 60%. As shown in Fig. 12a-e, the volumes of mesopores of coal samples with different moisture contents changed by  $-0.2966$ ,  $-0.263$ ,  $0.0289$ ,  $-0.4089$ , and  $-0.3363$ , respectively and the macropore volumes were changed by  $0.0863$ ,  $-0.1185$ ,  $-0.1092$ ,  $-0.0941$ , and  $0.1397$  after subcritical  $\text{CO}_2$  treatment, respectively. The seepage pore is composed of mesopores and macropores. Combined with

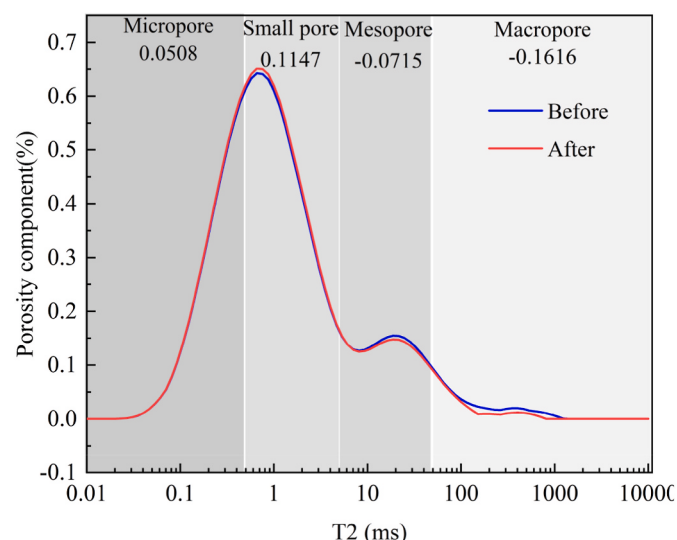


**Fig. 11.** T2 distribution of sample M.

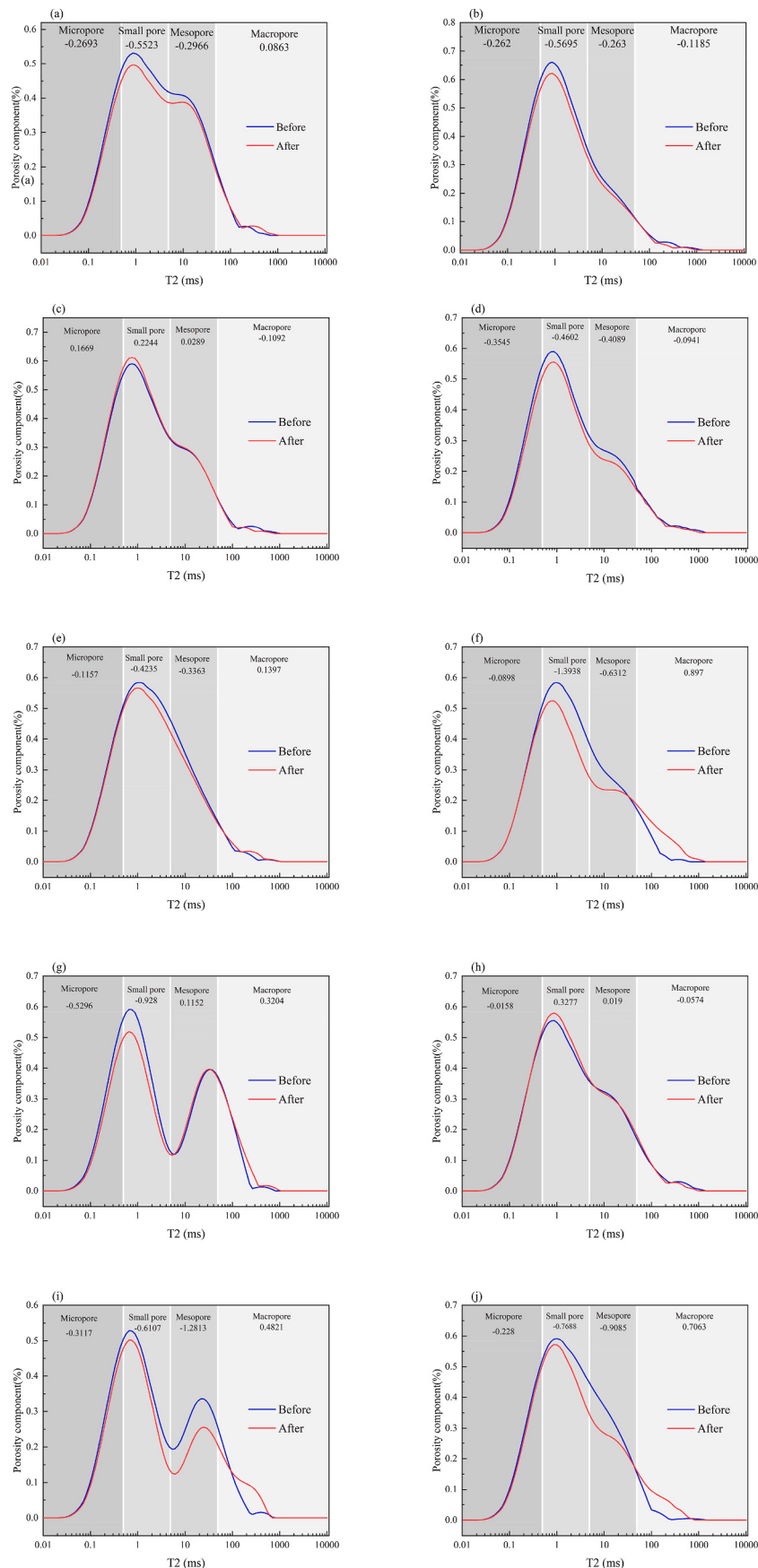


**Fig. 12.** T2 distribution of different coal samples before and after CO<sub>2</sub> treatment (a) 4 MPa + 0%, (b) 4 MPa + 2.8%, (c) 4 MPa + 5.6%, (d) 4 MPa + 8.4%, (e) 4 MPa + 11.2%, (f) 8 MPa + 0%, (g) 8 MPa + 2.8%, (h) 8 MPa + 5.6%, (i) 8 MPa + 8.4%, (j) 8 MPa + 11.2%.

the change of both, the volume change of seepage pore is: -0.2103, -0.3815, -0.0803, -0.503, -0.1966. The analysis shows that the volume change of macropores decreases at first and then increases. This is consistent with the change principle of coal sample permeability after subcritical CO<sub>2</sub> desorption (Fig. 8a). However, the change in seepage pore volume does not coincide with the change of the permeability after CO<sub>2</sub> desorption. The reason is that the permeability is mainly controlled by the macropores, while the drastic fluctuation of the mesopore volume causes the change of the seepage pore volume. Further analysis shows that the volume of the macropores of the coal samples decreases the most for a water content of 2.8%, reaching 0.1185, which does not exceed 0.1616 of the M group coal samples. Our results show that although subcritical CO<sub>2</sub> can increase the macropore volume and promote seepage, it cannot completely eliminate the effect during the loading and unloading process. Therefore, the permeability of coal samples decreases.

The T2 distributions of coal samples with different moisture contents after ScCO<sub>2</sub> treatment are shown in Fig. 12. The mesopore volumes of coal samples changed by -0.6312, 0.1152, 0.019, -1.2813, and -0.9085, and the macropore volumes by 0.897, 0.3204, -0.0574, 0.4821, and 0.7063, respectively after ScCO<sub>2</sub> treatment. A comparison with the pore changes after subcritical CO<sub>2</sub> desorption shows that the ScCO<sub>2</sub> adsorption has a stronger effect on the reformation of the coal sample pores. Based on the change characteristics of the seepage pores, it is evident that the increase of the seepage pore of coal sample attains the maximum for a water content of 2.8% after ScCO<sub>2</sub> desorption, which is consistent with the increase of the permeability of the coal sample with a water content of 2.8% (Fig. 7b). However, the seepage pores volume of the 8.4% and 11.2% moisture content coal samples decreases after CO<sub>2</sub> desorption, whereas the measured permeability increases. This discrepancy is induced by the increase in the volume of the macropores of the coal sample, whereas the large decrease in the mesopore volume causes the decrease of the overall seepage pore volume. It is thus indirectly constrained that the permeability of coal samples is mainly controlled by macropores. Different from the change trend of other coal samples, the seepage pore volume of the 5.6% moisture content coal sample decreases and the adsorption pore volume increases after ScCO<sub>2</sub> treatment, which is consistent with the permeability change (Fig. 8b) and findings in previous studies (Li et al., 2022).

Micropores and small pores are the main sites for CBM and CO<sub>2</sub> adsorption and storage. The analysis of the adsorption pores of coal samples before and after CO<sub>2</sub> treatment shows that the micropores and small pores of 5.6% moisture content coal samples changed by 0.1669 and 0.2244 respectively, after subcritical CO<sub>2</sub> treatment, and to -0.0158 and 0.3277 after ScCO<sub>2</sub> treatment. The volumes of micropores and small pores of the samples decrease. The results show that the CO<sub>2</sub> (subcritical and supercritical) treatment of the semi-saturated coal sample with water content of 5.6% will promote the development of micropores and small pores and thus provide more sites for CO<sub>2</sub> adsorption and storage. In order to better reveal the principle of pore reformation by CO<sub>2</sub> injection, XRD analysis was conducted on the coal samples before and after adsorption.

### 3.4. Mineral composition

The coal samples were analyzed by XRD, and the XRD data was semi-quantitatively processed with the Jade software. The mineral composition of coal is very complex, which means it's difficult to obtain the absolute content of minerals. Therefore, the paper analyzes the mechanism of changes in its pore structure by the relative content of main minerals contained in coal samples, which has been proved by many studies (Li et al., 2022; Niu et al., 2019). The results are summarized in Fig. 11 and document that the main mineral components of raw coal (RC) are: calcite (CaCO<sub>3</sub>) 25.2%, dolomite (CaMg(CO<sub>3</sub>)<sub>2</sub>) 5.53%, quartz (SiO<sub>2</sub>) 14.83%, pyrite (FeS<sub>2</sub>) 5.52%, and clay minerals (48.92%). The main clay minerals are illite (K<sub>3</sub>Fe<sub>4</sub>Si<sub>14</sub>Al<sub>7</sub>O<sub>40</sub>(OH)<sub>8</sub>) 33.11% and

kaolinite (Al<sub>2</sub>Si<sub>2</sub>O<sub>5</sub>(OH)<sub>4</sub>) 15.81%.

Fig. 13 shows that the content of carbonate minerals in the coal samples decreased to varying degrees after CO<sub>2</sub> treatment, which is related to the easy dissolution of carbonate minerals in an acidic environment (Du et al., 2018). The content of pyrite remains almost constant before and after treatment as pyrite is comparably stable. Although clay minerals were also dissolved, their contents slightly increase after CO<sub>2</sub> treatment due to their relatively slow reaction rate. Therefore, the higher relative content of clay minerals indicates enhanced dissolution of carbonate minerals. After subcritical CO<sub>2</sub> treatment, the content of clay minerals in coal samples increased from 49.08% to 67.78% as the moisture content increases, indicating that the degree of modification of minerals by CO<sub>2</sub> increases with the rise of moisture content. Thus, the permeability attenuation caused by the loading and unloading process is partially erased. However, dry coal has a lower clay mineral increase, indicating a small modification effect of CO<sub>2</sub>, although its permeability decay was minimal. The higher strength of dry coal and the reduced pore collapse during loading and unloading are proposed as main causes for this fact.

Correspondingly, the clay mineral content of coal samples is generally higher after supercritical CO<sub>2</sub> treatment, reflecting the more vigorous dissolution of carbonate minerals by supercritical CO<sub>2</sub>. The stronger corrosion ability is related to the higher CO<sub>2</sub> pressure and the lower solution pH (Perera, 2017). The clay minerals content of coal sample reaches a maximum of 69.92% for a moisture content of 2.8%, indicating that the carbonate minerals in the coal sample are almost completely dissolved and the pores are more thoroughly reformed. The clay mineral content of the 5.6% moisture content coal sample is 50.83%, which is a slight increase compared to RC. We propose that only part of the carbonate minerals was dissolved under the condition of such moisture content, and the modification of the pore was insufficient.

## 4. Discussion

### 4.1. Effect of mineral composition on pore structure

CO<sub>2</sub> will react with the water in the coal seam to generate carbonic acid when it is injected into the deep unexploitable coal seam (Jiang and Yu, 2019). Subsequently, carbonic acid is ionized to generate H<sup>+</sup>, which will promote a large amount of dissolution of carbonate minerals and clay minerals. The reaction mechanism is illustrated in Fig. 14.

A series of complex geochemical changes of minerals occur in the coal samples after ScCO<sub>2</sub> injection, resulting in changes of the mineral composition and pore structure. The specific reactions are as follows

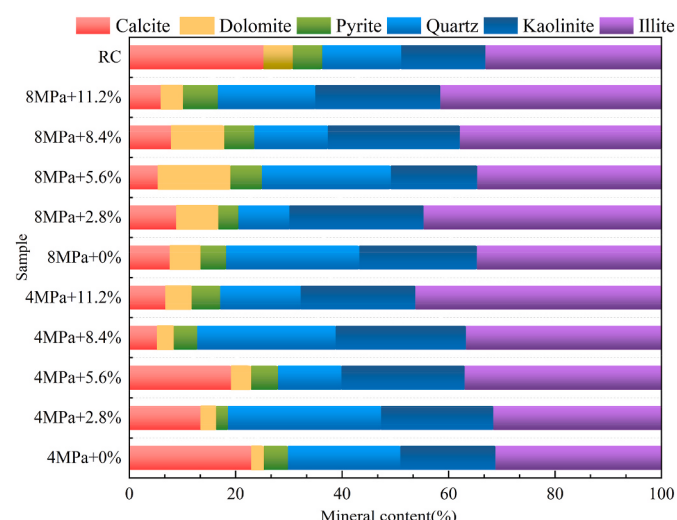


Fig. 13. Change of the mineralogy after CO<sub>2</sub> treatment.

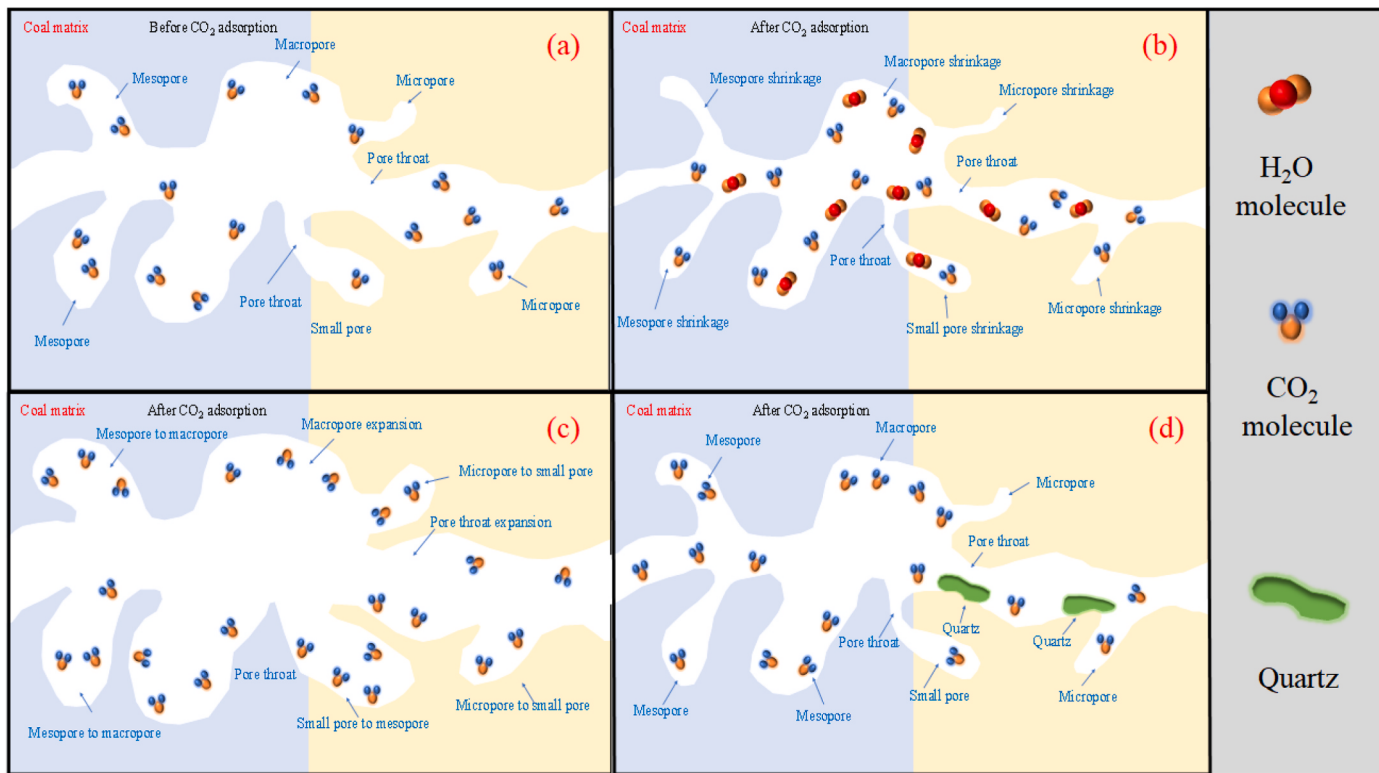
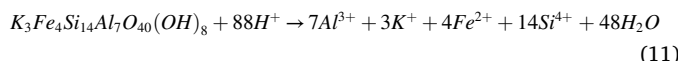
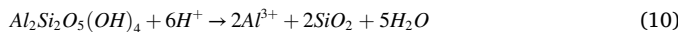
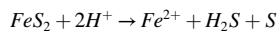
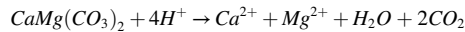
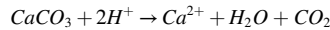
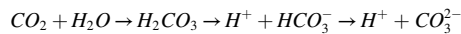


Fig. 14. Reaction mechanism.

(Ozotta et al., 2021; Z. Wang et al., 2021):



As shown in Fig. 14a, a large amount of  $H_2O$  molecules is distributed in the pores of coal samples. And then the expansion of coal matrix and clay minerals leads to pore shrinkage of coal samples after  $CO_2$  injection, which is shown in Fig. 14b.

The carbonate mineral dissolves fastest because it is most sensitive to acidic conditions when  $ScCO_2$  is injected into the coal sample (Du et al., 2018). And the dissolution rate increases with the increase of water content. On the one hand, the acidic environment formed by the reaction of water and  $CO_2$  to generate  $H_2CO_3$  promotes the dissolution reaction; On the other hand, the increase of water provides sufficient solution for  $Ca^{2+}$  and  $Mg^{2+}$  produced by carbonate dissolution, which promotes the forward progress of the reaction. Therefore, with the increase of water content, the dissolution rate of minerals in coal increases, which improves the pore connectivity and broadens the pore size, which is positive for seepage.

Compared with subcritical  $CO_2$ ,  $ScCO_2$  has a higher density, lower pH value, and a stronger ability of extraction and dissolution. As shown in Fig. 14c, the clay mineral content of 2.8% water content coal samples is the highest, which indicates that the dissolution of carbonate minerals is the most intense and the pores expand most. On contrast, the silicate minerals hardly dissolve, resulting in less quartz blocking the pores and

causing an ideal pore expansion and connectivity. The change of 5.6% water content coal samples after  $ScCO_2$  treatment is shown in Fig. 14d. Although  $CO_2$  also dissolves carbonate minerals and expands the pore volume of other moisture content coal samples, silicate minerals react vastly to form a large amount of quartz which may block the pore channels such as key pore throats, which is negative for the connectivity and expansion of pores.

The porosity of most water-bearing coal samples decreases after  $CO_2$  treatment, which is not consistent with previous research (Liu et al., 2010). This result is caused by the action of geochemical reaction and stress: (1) the expand of clay minerals and coal matrix compresses the pore channels; (2) The new mineral quartz produced by the dissolution of clay minerals precipitates in the pores and occupies the pore volume (Bo et al., 2023); (3) The stress in the  $CO_2$  treatment process compresses the coal sample and causes the pore shrinkage of the coal sample.

#### 4.2. Effect of pore structure on permeability

The pore structure has a direct and crucial impact on the permeability of the deep coal seam. The constrained geochemical reactions will largely transform the original pore structure of the coal seam when  $CO_2$  is injected into the coal seam. The NMR results show that the loading and unloading process will cause irreversible damage to the coal sample, which will lead to the transformation of mesopores and macropores to micropores and small pores. This transformation will result in a loss of permeability.

The macropore volume of the coal samples with different moisture contents decreases at first and subsequently increases after subcritical  $CO_2$  injection. Considering the loss of the macropore volume of M group coal samples by 0.1616 during the loading and unloading process, and the general decrease of the macropore volume of other coal samples that didn't exceed this range, it is evident that subcritical  $CO_2$  can improve the permeability of coal. However, this improvement cannot completely compensate the negative effect during loading and unloading due to its relatively weak effect on pore reformation. Therefore, the permeability

of coal samples after treatment is lower than the initial permeability. The change of the macropore volume decreased at first and then increased with the increase of coal sample moisture content. Although the permeability of coal is affected by the combination of mesopore and macropore, the effect of macropores is more important, documenting that the permeability change of coal samples exhibits the same trend as the change of macropore volume.

The macropore of all coal samples showed an increase after treatment with supercritical CO<sub>2</sub> (except for the coal samples with 5.6% moisture content) and the increase range was significantly higher than that of the subcritical CO<sub>2</sub>-treated coal samples. Combined with the change of the mesopore volume, the seepage pore volume of the coal sample with a moisture content of 2.8% increased at most (by 0.4356), followed by the dry coal with an increase of 0.2658. The data document that supercritical CO<sub>2</sub> has the strongest effect on the modification of seepage pores of coal samples with a water content of 2.8%, followed by dry coal, thereby promoting the improvement of coal sample permeability. Although macropores volume of the 8.4% water content and 11.2% water content coal samples increased stronger, the mesopores volume is significantly reduced, causing the overall seepage pore volume to decrease by 0.7992 and 0.2022, respectively, and reducing the pore connectivity. Therefore, their increase rates are lower than that of the former. The macropore volume of the 5.6% water content coal sample decreased whereas the mesopores slightly increased after ScCO<sub>2</sub> treatment, indicating that the permeability of the coal sample would decrease.

However, the adsorption pore volume of the 5.6% water content coal sample increased after CO<sub>2</sub> treatment, thus providing more sites for CO<sub>2</sub> adsorption. Moreover, the variation of the porosity is widely consistent with the variation trend of the permeability.

## 5. Conclusion

We conducted NMR, XRD, adsorption, and seepage analyses on coals samples with five different moisture contents before and after being treated with subcritical CO<sub>2</sub> and ScCO<sub>2</sub> to understand the effect of the moisture content on the pore structure, mineral compositions, and permeability of the CO<sub>2</sub>-treated coal samples. The following main conclusions were drawn from this study.

- (1) The coal sample expanded after CO<sub>2</sub> adsorption. The expansion of the coal sample caused by ScCO<sub>2</sub> is significantly stronger than that of the subcritical CO<sub>2</sub>. The increase of the moisture content inhibits the expansion of the coal samples by CO<sub>2</sub> adsorption due to the competitive adsorption of water and CO<sub>2</sub>.
  - (2) Subcritical CO<sub>2</sub> can increase the permeability of coal samples, but it cannot completely compensate the negative effects during the loading and unloading process, which is manifested as the attenuation of the permeability. The ScCO<sub>2</sub> can increase the permeability of coal samples significantly, e.g., the permeability of coal samples with 2.8% moisture content increases by up to 421.74% (for 8 MPa effective stress) and 2.8% is the ideal moisture content for permeability enhancement. In addition, the increase of the permeability of coal samples is intensified by the increase of the effective stress, indicating that ScCO<sub>2</sub> injection is specifically suited for permeability enhancement in deep coal seams.
  - (3) The results of NMR analysis show that subcritical CO<sub>2</sub> with weak solubility cannot completely eliminate the compression effect during loading and unloading, so the adsorption and permeation pore volumes of coal samples decrease, while ScCO<sub>2</sub> reaction is more intense, and the seepage pores of most coal samples increase. In addition, the pore transformation effect of coal samples presents M-type after ScCO<sub>2</sub> treatment with the increase of moisture content. And the transformation into macropores is the most at 2.8% water content, while the transformation from seepage pores to adsorption pores is the most at 5.6% water content. Thus, 5.6% is the ideal moisture content for geological CO<sub>2</sub> storage.
- (4) XRD analysis shows that carbonate minerals in coal samples are dissolved by acidic fluids formed by the reaction of CO<sub>2</sub> and H<sub>2</sub>O. The relative content of clay minerals increases due to the slow reaction, and the dissolution rate of the solution formed by subcritical CO<sub>2</sub> and H<sub>2</sub>O increases with the increase of moisture content. The solution formed by ScCO<sub>2</sub> and H<sub>2</sub>O has a strong solubility for coal samples, and its dissolution rate reaches a maximum when the water content is 2.8%.
- The conclusions provide a profound basis for simulating and predicting changes of the pore structure and permeability of coal seams with different water contents after CO<sub>2</sub> injection into deep unexploitable coal seams. The response of the remaining coal ranks to the water content will be the focus of subsequent studies.

## Author contributions

Ge ZL and Li CT conceived and designed the experiments; Li CT, Zhou Z, Zhang XY and Sheng MY performed the experiments; Li CT and Ge ZL analyzed the data; Li CT and Ge ZL contributed materials and analysis tools; Ge ZL, Li CT and Guan YR wrote the paper.

## Declaration of competing interest

The authors declare that they have no known competing financial interests or personal relationships that could have appeared to influence the work reported in this paper.

## Data availability

No data was used for the research described in the article.

## Acknowledgments

This study was financially supported by the National Natural Science Foundation of China (52074045), the Fundamental Research Funds for the Central Universities (2022CDJQY-008), the Graduate Research and Innovation Foundation of Chongqing, China (No. CYB21024).

## References

- Aminu, M.D., Nabavi, S.A., Rochelle, C.A., Manovic, V., 2017. A review of developments in carbon dioxide storage. *Appl. Energy* 208, 1389–1419.
- Bachu, S., 2008. CO<sub>2</sub> storage in geological media: role, means, status and barriers to deployment. *Prog. Energy Combust. Sci.* 34, 254–273.
- Bo, L., Jian, W., Junxiang, Z., Bo, W., Daohe, Z., 2023. Analysis of the change feature and action mechanism of coal pore structure under the action of supercritical CO<sub>2</sub>. *Int. J. Energy Res.* 8679917.
- Cai, Y., Liu, D., Pan, Z., Yao, Y., Li, J., Qiu, Y., 2013. Pore structure and its impact on CH<sub>4</sub> adsorption capacity and flow capability of bituminous and subbituminous coals from Northeast China. *Fuel* 103, 258–268.
- Cheng, Y., Zhang, X., Lu, Z., Pan, Z. jun, Zeng, M., Du, X., Xiao, S., 2021. The effect of subcritical and supercritical CO<sub>2</sub> on the pore structure of bituminous coals. *J. Nat. Gas Sci. Eng.* 94.
- Cui, G., Yang, L., Fang, J., Qiu, Z., Wang, Y., Ren, S., 2021. Geochemical reactions and their influence on petrophysical properties of ultra-low permeability oil reservoirs during water and CO<sub>2</sub> flooding. *J. Petrol. Sci. Eng.* 203.
- Danesh, N.N., Chen, Z., Connell, L.D., Kizil, M.S., Pan, Z., Aminossadati, S.M., 2017. Characterisation of creep in coal and its impact on permeability: an experimental study. *Int. J. Coal Geol.* 173, 200–211.
- Du, Y., Fu, C., Pan, Z., Sang, S., Wang, W., Liu, S., Zhao, Y., Zhang, J., 2020. Geochemistry effects of supercritical CO<sub>2</sub> and H<sub>2</sub>O on the mesopore and macropore structures of high-rank coal from the Qinshui Basin, China. *Int. J. Coal Geol.* 223 <https://doi.org/10.1016/j.coal.2020.103467>.
- Fujioka, M., Yamaguchi, S., Nako, M., 2010. CO<sub>2</sub>-ECBM field tests in the ishikari coal basin of Japan. *Int. J. Coal Geol.* 82, 287–298.
- Gao, S., Jia, L., Zhou, Q., Cheng, H., Wang, Y., 2022. Microscopic pore structure changes in coal induced by a CO<sub>2</sub>-H<sub>2</sub>O reaction system. *J. Petrol. Sci. Eng.* 208.

- Gunter, W.D., Gentzis, T., Rottenfusser, B.A., Richardson, R.J.H., 1997. Deep coalbed methane in Alberta, Canada: a fuel resource with the potential of zero greenhouse gas emissions. *Energy Convers. Manag.* 38, S217–S222.
- Guo, P., Cheng, Y., Jin, K., Li, W., Tu, Q., Liu, H., 2014. Impact of effective stress and matrix deformation on the coal fracture permeability. *Transport Porous Media* 103, 99–115. <https://doi.org/10.1007/s11242-014-0289-4>.
- Hao, D., Zhang, L., Li, M., Tu, S., Zhang, C., Bai, Q., Wang, C., 2018. Experimental study of the moisture content influence on  $\text{CH}_4$  adsorption and deformation characteristics of cylindrical bituminous coal core. *Adsorpt. Sci. Technol.* 36, 1512–1537. <https://doi.org/10.1177/0263617418788444>.
- Hu, Z., Li, C., Zhang, D., 2021. Interactions of dynamic supercritical  $\text{CO}_2$  fluid with different rank moisture-equilibrated coals: implications for  $\text{CO}_2$  sequestration in coal seams. *Chin. J. Chem. Eng.* 35, 288–301.
- Huang, L., Ning, Z., Wang, Q., Zhang, W., Cheng, Z., Wu, X., Qin, H., 2018. Effect of organic type and moisture on  $\text{CO}_2/\text{CH}_4$  competitive adsorption in kerogen with implications for  $\text{CO}_2$  sequestration and enhanced  $\text{CH}_4$  recovery. *Appl. Energy* 210, 28–43.
- Jasinge, D., Ranjith, P.G., Choi, X., Fernando, J., 2012. Investigation of the influence of coal swelling on permeability characteristics using natural brown coal and reconstituted brown coal specimens. *Energy* 39, 303–309.
- Jiang, R., Yu, H., 2019. Interaction between sequestered supercritical  $\text{CO}_2$  and minerals in deep coal seams. *Int. J. Coal Geol.* 202, 1–13.
- Jin, Z., Wu, S., Deng, C., Dai, F., 2017.  $\text{H}_2\text{O}$  adsorption mechanism in coal basing on Monte Carlo method. *J. China Coal Soc.* 42, 2968–2974.
- Leung, D.Y.C., Caramanna, G., Maroto-Valer, M.M., 2014. An overview of current status of carbon dioxide capture and storage technologies. *Renew. Sustain. Energy Rev.* 39, 426–443.
- Li, W., Liu, Z., Su, E., Cheng, Y., 2019. Experimental investigation on the effects of supercritical carbon dioxide on coal permeability: implication for  $\text{CO}_2$  injection method. *Energy Fuel.* 33, 503–512. <https://doi.org/10.1021/acs.energyfuels.8b03729>.
- Li, R., Ge, Z., Wang, Z., Zhou, Z., Zhou, J., Li, C., 2022. Effect of supercritical carbon dioxide ( $\text{ScCO}_2$ ) on the microstructure of bituminous coal with different moisture contents in the process of  $\text{ScCO}_2$  enhanced coalbed methane and  $\text{CO}_2$  geological sequestration. *Energy Fuel.* 36, 3680–3694.
- Liu, C.J., Wang, G.X., Sang, S.X., Rudolph, V., 2010. Changes in pore structure of anthracite coal associated with  $\text{CO}_2$  sequestration process. *Fuel* 89, 2665–2672.
- Liu, Z., Liu, D., Cai, Y., Yao, Y., Pan, Z., Zhou, Y., 2020. Application of nuclear magnetic resonance (NMR) in coalbed methane and shale reservoirs: a review. *Int. J. Coal Geol.* 218 <https://doi.org/10.1016/j.coal.2019.103261>.
- Liu, S., Yuan, L., Zhao, C., Zhang, Y., Song, Y., 2022. A review of research on the dispersion process and  $\text{CO}_2$  enhanced natural gas recovery in depleted gas reservoir. *J. Petrol. Sci. Eng.* 208.
- Massarotto, P., Golding, S.D., Bae, J.S., Iyer, R., Rudolph, V., 2010. Changes in reservoir properties from injection of supercritical  $\text{CO}_2$  into coal seams-A laboratory study. *Int. J. Coal Geol.* 82, 269–279.
- Mazzotti, M., Pini, R., Storti, G., 2009. Enhanced coalbed methane recovery. *J. Supercrit. Fluids* 47, 619–627.
- Meng, Z., Li, G., 2013. Experimental research on the permeability of high-rank coal under a varying stress and its influencing factors. *Eng. Geol.* 162, 108–117. <https://doi.org/10.1016/j.enggeo.2013.04.013>.
- Meng, Y., Li, Z., Lai, F., 2015. Experimental study on porosity and permeability of anthracite coal under different stresses. *J. Petrol. Sci. Eng.* 133, 810–817.
- Niu, Q., Cao, L., Sang, S., Zhou, X., Wang, Z., Wu, Z., 2017. The adsorption-swelling and permeability characteristics of natural and reconstituted anthracite coals. *Energy* 141, 2206–2217.
- Niu, Q., Cao, L., Sang, S., Zhou, X., Wang, Z., 2018. Anisotropic adsorption swelling and permeability characteristics with injecting  $\text{CO}_2$  in coal. *Energy Fuel.* 32, 1979–1991.
- Niu, Q., Cao, L., Sang, S., Zhou, X., Liu, S., 2019. Experimental study of permeability changes and its influencing factors with  $\text{CO}_2$  injection in coal. *J. Nat. Gas Sci. Eng.* 61, 215–225. <https://doi.org/10.1016/j.jngse.2018.09.024>.
- Ozotta, O., Ostadhassan, M., Liu, K., Liu, B., Kolawole, O., Hadavimoghaddam, F., 2021. Reassessment of  $\text{CO}_2$  sequestration in tight reservoirs and associated formations. *J. Petrol. Sci. Eng.* 206.
- Pashin, J.C., Clark, P.E., McIntyre-Redden, M.R., Carroll, R.E., Esposito, R.A., Oudinot, A.Y., Koperna, G.J., 2015. SECARB  $\text{CO}_2$  injection test in mature coalbed methane reservoirs of the Black Warrior Basin, Blue Creek Field, Alabama. *Int. J. Coal Geol.* 144 (145), 71–87.
- Perera, M.S.A., 2017. Influences of  $\text{CO}_2$  injection into deep coal seams: a review. *Energy Fuel.* 31, 10324–10334.
- Perera, M.S.A., Ranjith, P.G., Choi, S.K., Airey, D., 2011. The effects of sub-critical and super-critical carbon dioxide adsorption-induced coal matrix swelling on the permeability of naturally fractured black coal. *Energy* 36, 6442–6450.
- Shi, J.Q., Durucan, S., Shimada, S., 2014. How gas adsorption and swelling affects permeability of coal: a new modelling approach for analysing laboratory test data. *Int. J. Coal Geol.* 128–129, 134–142.
- Song, Y., Zou, Q., Su, E., Zhang, Y., Sun, Y., 2020. Changes in the microstructure of low-rank coal after supercritical  $\text{CO}_2$  and water treatment. *Fuel* 279.
- Talapatra, A., Karim, M.M., 2020. The influence of moisture content on coal deformation and coal permeability during coalbed methane (CBM) production in wet reservoirs. *J. Pet. Explor. Prod. Technol.* 10, 1907–1920.
- Teng, T., Gao, F., Ju, Y., Xue, Y., 2017. How moisture loss affects coal porosity and permeability during gas recovery in wet reservoirs? *Int. J. Min. Sci. Technol.* 27, 899–906.
- Wang, K., Du, F., Wang, G., 2017. Investigation of gas pressure and temperature effects on the permeability and steady-state time of Chinese anthracite coal: an experimental study. *J. Nat. Gas Sci. Eng.* 40, 179–188.
- Wang, X., Deng, C., Qiao, L., Chu, G., Jing, R., Kang, Y., 2021. A study on factors influencing  $\text{CO}_2$  adsorption by coal. *AIP Adv.* 11 (3), 035238.
- Wang, Z., Ge, Z., Li, R., Zhou, Z., Hou, Y., Zhang, H., 2021. Coupling effect of temperature, gas, and viscoelastic surfactant fracturing fluid on the microstructure and its fractal characteristics of deep coal: an experimental study. *Energy Fuel.* 35, 19423–19436. <https://doi.org/10.1021/acs.energyfuels.1c02809>.
- Wang, Z., Ge, Z., Li, R., Zhou, Z., Hou, Y., Zhang, H., 2022. Coupling effect of temperature, gas, and viscoelastic surfactant fracturing fluid on the chemical structure of deep coal: an experimental study. *Energy Fuel.* 36, 3468–3480. <https://doi.org/10.1021/acs.energyfuels.1c03796>.
- Wong, S., Law, D., Deng, X., Robinson, J., Kadatz, B., Gunter, W.D., Jianping, Y., Sanli, F., Zhiqiang, F., 2007. Enhanced coalbed methane and  $\text{CO}_2$  storage in anthracitic coals-Micro-pilot test at South Qinshui, Shanxi, China. *Int. J. Greenh. Gas Control* 1, 215–222.
- Xu, J., Zhai, C., Liu, S., Qin, L., Wu, S., 2017. Pore variation of three different metamorphic coals by multiple freezing-thawing cycles of liquid  $\text{CO}_2$  injection for coalbed methane recovery. *Fuel* 208, 41–51.
- Zhang, Z., Huisingh, D., 2017. Carbon dioxide storage schemes: technology, assessment and deployment. *J. Clean. Prod.* 142, 1055–1064.
- Zhang, K., Sang, S., Liu, C., Ma, M., Zhou, X., 2019. Experimental study the influences of geochemical reaction on coal structure during the  $\text{CO}_2$  geological storage in deep coal seam. *J. Petrol. Sci. Eng.* 178, 1006–1017.
- Zhang, H., Hu, Z., Xu, Y., Fu, X., Li, W., Zhang, D., 2021. Impacts of long-term exposure to supercritical carbon dioxide on physicochemical properties and adsorption and desorption capabilities of moisture-equilibrated coals. *Energy Fuel.* 35, 12270–12287.
- Zhu, C. jie, Liu, N., Gao, Z. shan, Hu, S. jia, Zhao, P. yuan, Liu, T., 2020. Experimental comparison of  $\text{CO}_2$ ,  $\text{N}_2$ , and  $\text{CH}_4$  permeability of water saturated coals of different ranks. *Energy Sources, Part A Recovery, Util. Environ. Eff.* 1 (13).